Journal of Institute of Science and Technology, 30(2), 151-162 (2025)
ISSN: 2467-9062 (print), e-ISSN: 2467-9240
https://doi.org/10.3126/jist.v30i2.84761

Research Article

EFFICIENCY OF BIOMASS-DERIVED ACTIVATED CARBON FOR RIVER WATER TREATMENT

Mandira Pradhananga Adhikari[1*], Dhurba Suwal[1], Nanda Bikram Adhikari[2*]
[1]Central Department of Chemistry, Tribhuvan University; 44613 Kirtipur, Kathmandu, Nepal
[2]Department of Electronics and Computer Engineering, Pulchowk Campus, 44600, Pulchowk, Lalitpur, Nepal
**Corresponding author:* mandira43@hotmail.com/ *mandira.pradhananga@cdc.tu.edu.np/* adhikari@ioe.edu.np

***(Received:** September 23, 2025; **Revised:** December 9, 2025; **Accepted:** December 12, 2025)*

ABSTRACT

Eliminating pollutants using activated carbon is one of the economic and efficient solutions to address the water scarcity problem. Biomass-derived nanoporous activated carbons (ACs) were prepared from *Buddleja* wood powder with phosphoric acid activation and characterized by methylene blue and iodine adsorption, Boehm titration, and point of zero charge. Further ACs were characterized using advanced instrumental analysis, such as Scanning Electron Microscopy (SEM), Raman scattering, and Fourier Transform Infrared Spectroscopy (FTIR). The maximum adsorption of iodine (667.0 mg/g) and methylene blue (140.84 mg/g) was observed at the ratio of 1:2 (precursor: phosphoric acid, BWC_2.0). The optimum conditions for adsorbing methylene blue were pH 10, 120 min contact time, adsorbent dose 1.6 g/L, and 100 mg/L methylene blue concentration. The BWC_2.0 turned the black color of the river water to colorless and reduced most of the contaminants to less than 20 %. Most of the pollutants, such as turbidity, oxidation-reduction potential (ORP), acidity, alkalinity, hardness, sulphate, phosphate, nitrate, iron, and chromium, are removed by more than 70% and chloride by 61%. The results implied that the *Buddleja* wood-derived activated carbon is useful in reducing pollutants from extremely polluted river water. In addition to adsorption of methylene blue from synthetic water, it works efficiently in the removal of pollutants from natural river water.

Keywords: Bagmati River, Buddleja wood, Isotherm, Methylene blue, Phosphoric acid

INTRODUCTION

Clean and safe water is essential for the survival of living organisms, including humans (Mutlu & Kurnaz, 2017). The quality of water resources such as rivers, ponds, and lakes has been deteriorating continuously due to unmanaged urbanization and direct discharge of industrial effluents and untreated sewage into water bodies, in addition to inadequate wastewater treatment. The Bagmati River is one of the historically, culturally, hydrologically, and geographically significant rivers in the river system in Nepal. Recent studies on water quality suggested severe contamination in this river, particularly in the densely populated capital of Nepal. Current studies reported that the water quality of this river frequently exceeds the safe limits of World Health Organization (WHO) standards (Adhikari *et al*., 2024; Sharma *et al.*, 2011). It was mentioned that human health may be at risk if contaminated river water is used. The studies suggest that treatment of river water is enormously important to protect public health and to address the scarcity of water.

Commonly used techniques for the purification of water comprise the coagulation, precipitation, and flocculation stages, which employ the synthetic chemicals (coagulants) to remove dissolved and suspended harmful contaminants (Alazaiza *et al*., 2022; Sathish *et al*., 2018). The chemical coagulants can remove dissolved and suspended contaminants; however, they are expensive, inefficient, and/or release excess sludge that requires further management (Alazaiza *et al*., 2022; Sathish *et al*., 2018; Tsolaki & Diamadopoulos, 2010). Hence, the use of natural sources is an efficient and sustainable solution (Dias *et al*., 2021; Tsolaki & Diamadopoulos, 2010). Recently, activated carbons from agricultural products have been used extensively in water treatment due to their efficient adsorbing capacity (Bhatnagar *et al.*, 2013; Kakom *et al*., 2023). The adsorbing efficiency depends on surface functional groups and pore structure of activated carbon. The characteristics of pores on the surface of activated carbon are influenced by several factors, namely activation temperature, methods, duration, activating agent, impregnation ratio, and carbonization duration (Adhikari & Thapa, 2020; Hendrawan *et al.*, 2019). The availability of functional groups depends on the constituents of the activating agents and the precursor. Several acids, bases, and salts are used as activating

agents. Among these, phosphoric acid is used as an activating agent in this study due to its lower toxicity, easy recoverability, and effective pore-developing capability (Megherbi *et al*., 2025). The low-cost activated carbons from agricultural waste materials have been the subject of research interest for water treatment (Kakom *et al*., 2023; Kuok *et al*., 2024). *Buddleja asiatica*, commonly known as the Asian butterfly bush, is a species of flowering shrub native to Asia, including Nepal, India, and China. It is a deciduous shrub abundantly found in sloping and forest areas in Nepal (Turin, 2003). *Buddleja* wood consists of high volatile matter and low ash, suitable for a precursor; there are limited studies on activated carbons, especially for the treatment of polluted natural river water.

The novelty of this study is the use of agricultural waste *Buddleja* wood as a low-cost precursor for the first time to synthesize activated carbons (BWCs) using phosphoric acid as an activator. The objective of this study is to optimize the doses of phosphoric acid to develop porosity on the surface of the activated carbon and efficiently treat synthetic water containing dye and natural river water. To fulfill the objective, the most efficient activated carbon prepared using a 1:2 ratio of precursor to activating agent (BWC_2.0) was utilized for the treatment of heavily polluted river water instead of the mostly used synthetic water. The results suggested that the BWC_2.0 efficiently reduced contaminants from extremely polluted river water.

MATERIALS AND METHODS

Activated Carbon from *Buddleja* Wood Powder

Locally available, clean, and dried *Buddleja* wood powder was chemically activated by treating it with different amounts of 65% H_3PO_4 (an activating agent). After 24 hours of chemical treatment, the mixture was transferred to a tube furnace for carbonization in an inert atmosphere at 400°C for three hours. The carbonized mixture was crushed and sieved using a mesh of 400 micrometers in size, then washed with dilute NaOH to neutralize the acid. *Buddleja* wood activated carbons were represented by BWC_1.0, BWC_1.5, BWC_2.0, and BWC_4.0. The number indicated the weight of the phosphoric acid used in terms of precursor.

Characterization of *Buddleja* Activated Carbons (BWCs)

The porosity developed after activation of *Buddleja* wood powder was characterized using iodine and methylene blue adsorption (Adhikari & Thapa, 2020). The iodine number was calculated using the following equation 1.

$$Iodine\ number = \frac{Amount\ of\ iodine\ adsorbed\ (mg)}{Weight\ of\ activated\ carbon\ (g)} \quad \ldots (1)$$

The methylene blue number was determined using a multipoint adsorption isotherm. Equation 2 was used to determine the quantity of methylene blue adsorbed by the activated carbon.

$$MB_N = \frac{(C_o - C_e)V}{M} \ldots (2)$$

Where C_o and C_e are the initial and equilibrium concentrations of methylene blue (mg/L), respectively. The V is the volume (L) of methylene blue, and the M is the mass (g) of activated carbon.

From the isoelectric point (point of zero charge, pH_{zpc}), the positive and negative charge availability on the surface of the activated carbon was evaluated (Sing, 1982). From the Boehm titrations, the acidic and basic surface functional groups of the activated carbon were quantified (Boehm, 1994). The thermogravimetric analysis (TGA) was conducted using a STA 2500 (Regulus, NETZSCH, Germany). The qualitative analysis of surface functional groups was performed using Fourier Transform Infrared (FTIR) spectroscopy (NICOLET iS20, Thermo-Fisher Scientific, Waltham, MA, USA). Raman scattering spectroscopy (NRS-3100, JASCO, Tokyo, Japan) was used for the determination of graphitic and defective carbons (Adhikari *et al*., 2025). The surface morphology of an adsorbent was evaluated by Scanning Electron Microscope (SEM) (S-4800, Hitachi Co., Ltd., Tokyo, Japan) operated at 10 kV and 10 μA) (Adhikari *et al*., 2025).

Application of Activated Carbon (BWC_2.0)

The methylene blue adsorption mechanism was studied using both the Langmuir and the Freundlich adsorption isotherms. The Langmuir adsorption model (linearized) is denoted as,

$$\frac{C_e}{q_e} = \frac{1}{q_{max}\, b} + \left(\frac{1}{q_{max}}\right) C_e \ldots (3)$$

Where C_e (mg/L) is the concentration at equilibrium, q_{max} and q_e are the maximum and equilibrium concentration of methylene blue adsorbed by one gram of adsorbent (mg/g), b (L/mg) is the Langmuir constant, calculated from C_e/q_e versus C_e curve. The parameter b was applied in equation 2 to calculate the equilibrium parameter (R_L) for the determination of the Langmuir isotherm applicability

$$R_L = \frac{1}{1 + bC_o} \quad \ldots (2)$$

The Freundlich adsorption isotherm (linearized) is

$$logq_e = logK_F + \left(\frac{1}{n}\right) logC_e \quad \ldots (3)$$

Herein, q_e is x/m, x is the amount of adsorbate (mg) adsorbed, m is the weight of adsorbent (g), K_F (mg/g) is the adsorption capacity, and n is the Freundlich adsorption intensity.

The removal efficiency of pollutants from heavily polluted Bagmati River water was studied by treating it with *Buddleja* wood-derived activated carbon (BWC_2.0). The sample was collected from Balkhu (27.68N, 85.30E), one of the heavily polluted areas in the valley, in the winter season, following the standard procedure (Adhikari *et al*., 2024). The water quality parameters, such as temperature, *pH*, DO, oxidation-reduction potential (ORP), turbidity, conductivity, total dissolved solids (TDS), and salinity were measured and recorded by using a portable multi-parameter analyzer (Hi-9829, HANNA instruments, Woonsocket, USA)., hardness, alkalinity, and chloride, were determined titrimetrically, phosphate, sulfate, iron, and chromium ion concentrations, were determined using a spectrophotometer (UV/VIS Spectrophotometer, DRAWEL, DV8200, Chongqing, China) before and after treatment with activated carbon. Sulfate was determined from the turbidity method, and phosphate was determined from the molybdenum blue method (APHA, 2012; Lund, 2019).

RESULTS AND DISCUSSION

The proximate analysis characterized the constituents of precursors. It shows that *Buddleja* wood powder consists of 12.56% moisture, 68.98% volatile substances, 16.19% fixed carbon, and 2.27% ash. 16.19 % of fixed carbon with a low ash content indicated that the precursor can be used to develop porous activated carbon. The thermal behaviour of *Buddleja* wood powder (BWP) was analyzed using the thermogravimetric (TG) curve from 25 – 800°C, as shown in Figure 1. The TG curve shows that until 200°C the minimal weight loss occurred, indicating a lower moisture content. The major mass reduction, more than 60%, occurred between 200 to 400°C, suggesting the evaporation of organic compounds from *Buddleja* wood powder. About 5% mass reduction occurred between 400 to 700°C. Above 700°C, the % mass reduction was insignificant. The weight loss was more clearly observed in derivative thermogravimetric (DTG) analysis. The small peak at 100°C represents the weight lost due to evaporation of moisture. A large and broad peak between 250 and 400°C shows the significant weight lost due to the degradation of cellulose and lignin, and the decomposition of hemicellulose (Adhikari & Thapa, 2020; Carrier *et al*., 2011; Saka, 2012; Shin *et al*., 1997;). Considering the lack of peaks on the DTG curve above 400°C (Figure 1), phosphoric acid impregnated *Buddleja* wood powder was carbonized at 400°C to synthesize a porous structure on the activated carbon.

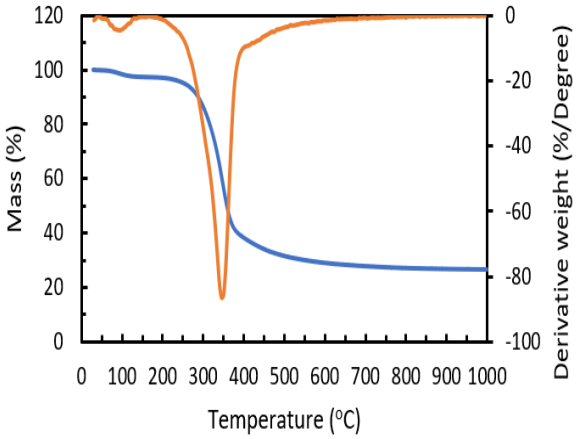

Figure 1: Thermogravimetric analysis (TGA) and derivative thermogravimetric (DTG) curves of *Buddleja* wood powder.

The adsorption capacity is a key indicator for evaluating the performance of activated carbon in removing contaminants or pollutants from water. Commonly, iodine and methylene blue adsorption determine the adsorptive capacity of activated carbon.

The methylene blue and iodine numbers (mg/g) are a relative guideline for measuring mesoporosity (methylene blue number) and microporosity (iodine number) of activated carbon (Adhikari & Thapa, 2020; Saka, 2012). The amount of iodine and methylene blue absorbed by different activated carbons was plotted in Figure 2. Both methylene blue and iodine numbers increased with an increase in phosphoric acid up to the 1:2.0 ratio and decreased with further increase in phosphoric acid. The dependence of iodine and methylene blue adsorption on the ratio is an indication of the dependency of the activating agent in the development of pores on the surface of activated carbons.

(a)

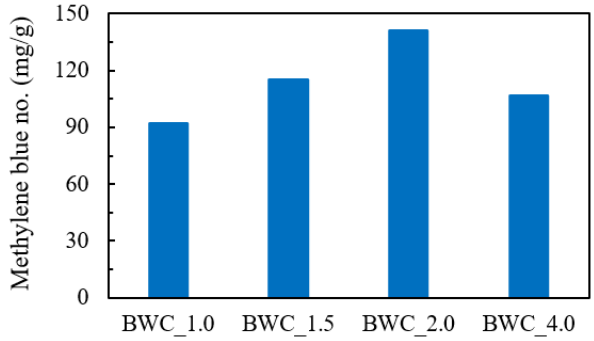

(b)

Figure 2. (a) Iodine number, and (b) methylene blue number of *Buddleja* wood-derived activated carbons at different impregnation ratios

The highest value of iodine number (667 mg/g, Figure 2a) and methylene blue number (140 mg/g, Figure 2b) were observed for BWC_2.0. The phosphoric acid reacts more extensively and completely with the surface of carbon at a 1:2.0 ratio of precursor to phosphoric acid (BWC_2.0) (Saka, 2012).

The surface functional group is an additional factor that influences the adsorption capacity, as adsorption phenomena occur on the surface of activated carbon. The qualitative analysis of the functional groups was determined from Fourier Transform Infrared (FTIR) Spectroscopy (Figure 3a). The broad and intense peak in the 3200-3600 cm^{-1} range suggests the stretching vibrations of the OH group into intermolecular hydrogen bonding (Adhikari *et al.*, 2025). The stretching of asymmetrical C-H was represented by the peak at 2916 cm^{-1} (Saka, 2012). The distinct peaks at 1614 and 1069 cm^{-1} refer to the N-H bending (amine) and stretching (C-O) vibration of the carboxylate groups (Shin *et al*., 1997). The quantitative analysis of acidic (lactonic, carboxylic, and phenolic) and basic functional groups of BWC_2.0 was carried out using Boehm titration (Boehm, 1994). BWC_2.0 consists of carboxylic (0.225 mmole/g), lactonic (0.450 mmole/g), and phenolic (1.274 mmole/g) groups (Table 1).

Table 1: Functional group concentration and point of zero charge of BWC_2.0.

Parameter	BWC_2.0
Phenolic group (mmole/g)	1.274
Lactonic group (mmole/g)	0.450
Carboxylic group (mmole/g)	0.225
Basic group (mmole/g)	0.162
pH_{pzc}	6.85

The basic functional group observed was about 0.162 mmol/g in BWC_2.0. The concentration of phenolic groups was a maximum among the acid group, which is consistent with the intense peak of the OH functional group observed in the FTIR spectra. The small but similar peaks of carboxylic and amino groups in the spectrum were verified by the comparable concentration of carboxylic and basic groups from the Boehm titration. The FTIR spectrum and Boehm titration indicated the presence of carboxylic and hydroxyl groups on the surface of BWC_2.0, which will be applicable to remove contaminants from water. These carboxyl and hydroxyl groups interact with positively charged ions, whereas amino groups interact with negatively charged ions from polluted river water during treatments (Pereira *et al.*, 2003). The point of zero charge (pH_{zpc}, Figure 3b) also gives information about the surface charge of the activated carbon (Adhikari *et al.*, 2025). When the *pH* is less than $pH_{zpc,}$ the protonation of surface functional groups occurs, and the surface becomes positively charged. At a *pH* higher than the pH_{zpc} value, due to deprotonation of the surface functional groups, the surface becomes negatively charged. The pH_{pzc} value (6.85) indicated that when the *pH* is lower than 6.85, the positively charged surface adsorbs negatively charged anions electrostatically. When the *pH* is higher than 6.85, the surface is negatively charged and adsorbs cations (Sing, 1982).

The various structural forms of carbon were studied by using Raman spectra. The intensity, position, and width of the peaks give information on the structural properties of carbon. The amorphous carbon usually shows broad peaks at around 1614 and 1360 cm^{-1}, representing first-order Raman spectra. These peaks are the characteristic peaks of disordered carbon (D) and graphitic carbon (G). The Raman spectra of BWCs showed the D and G bands at 1380 and 1597 cm^{-1}, respectively (Figure 3c) (Adhikari *et al.*, 2025; Vali *et*

al., 2024). The intensity ratio of G and D bands in BWC_2.0 was 1.23. The intensity ratio (I_G/I_D) describes the structural disorder, the size of sp^2 clusters, and the ratio of sp^3 to sp^3 bonding in hydrogenated amorphous carbons (Vali *et al*., 2024). The G-band is related to the sp^2 bond stretching in chains and rings, and the D-band is related to the sp^2 atoms in rings. The peak of the D band suggests the defect in activated carbon, and the peak of the G band suggests the graphitic structure (Pradhananga *et al*., 2017; Vali *et al*., 2024). The ratio of I_G/I_D (1.23) in the Raman spectra of BWC_2.0 suggests that defects were introduced during the activation process (Adhikari *et al*., 2025; Vali *et al*., 2024). The broad peak suggests amorphous particles and a high value of the ratio I_G/I_D, i.e., a small D band, indicates the introduction of fewer defects during activation and carbonization (Yuan *et al*., 2025).

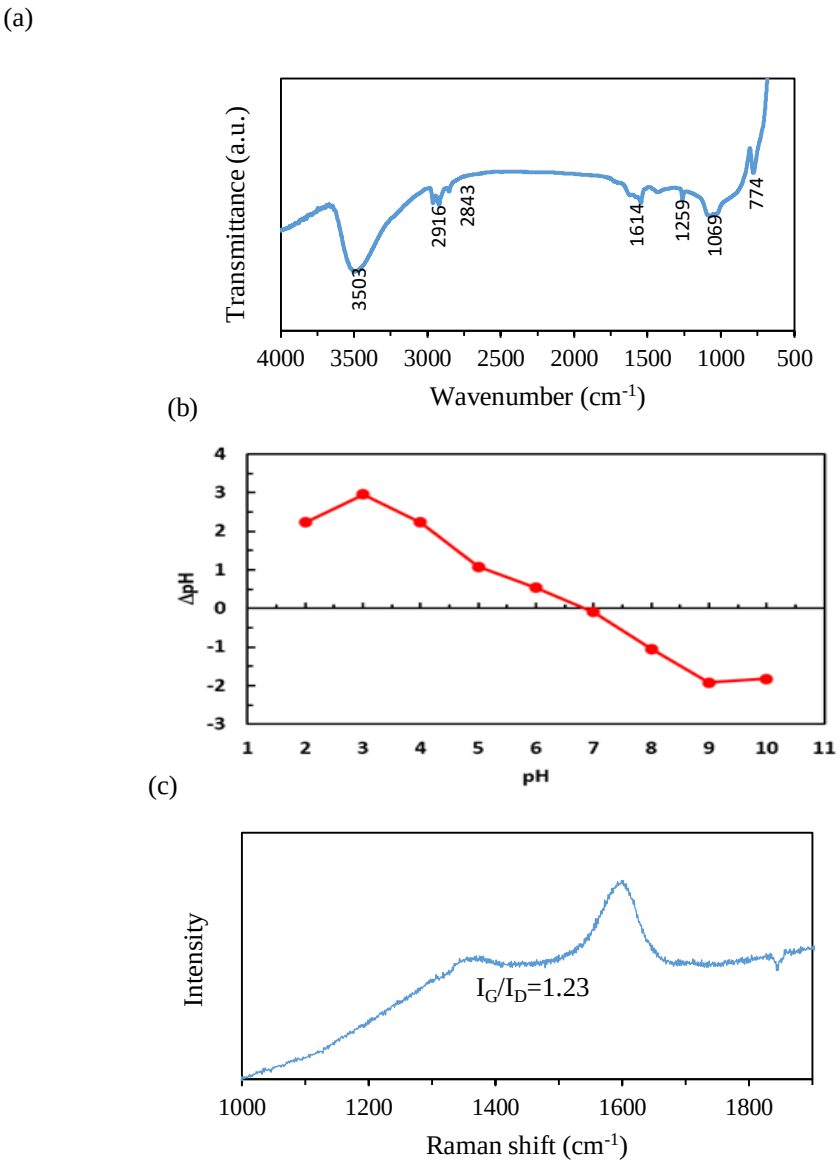

Figure 3. (a) FTIR (b) point of zero charge (pH_{pzc}) and (c) Raman spectra of BWC-2.0.

The SEM images of BWC_2.0 captured at varying magnifications are shown in Figure 4. Laminar structures with irregular sizes are observed in Figure 4a, indicating the amorphous activated carbon. Figure 4b and 4c show granular particles with different shapes and sizes containing pores with sizes less than 1 µm, which is quite expected as the materials were prepared by H_3PO_4 activation of precursors without using any templates.

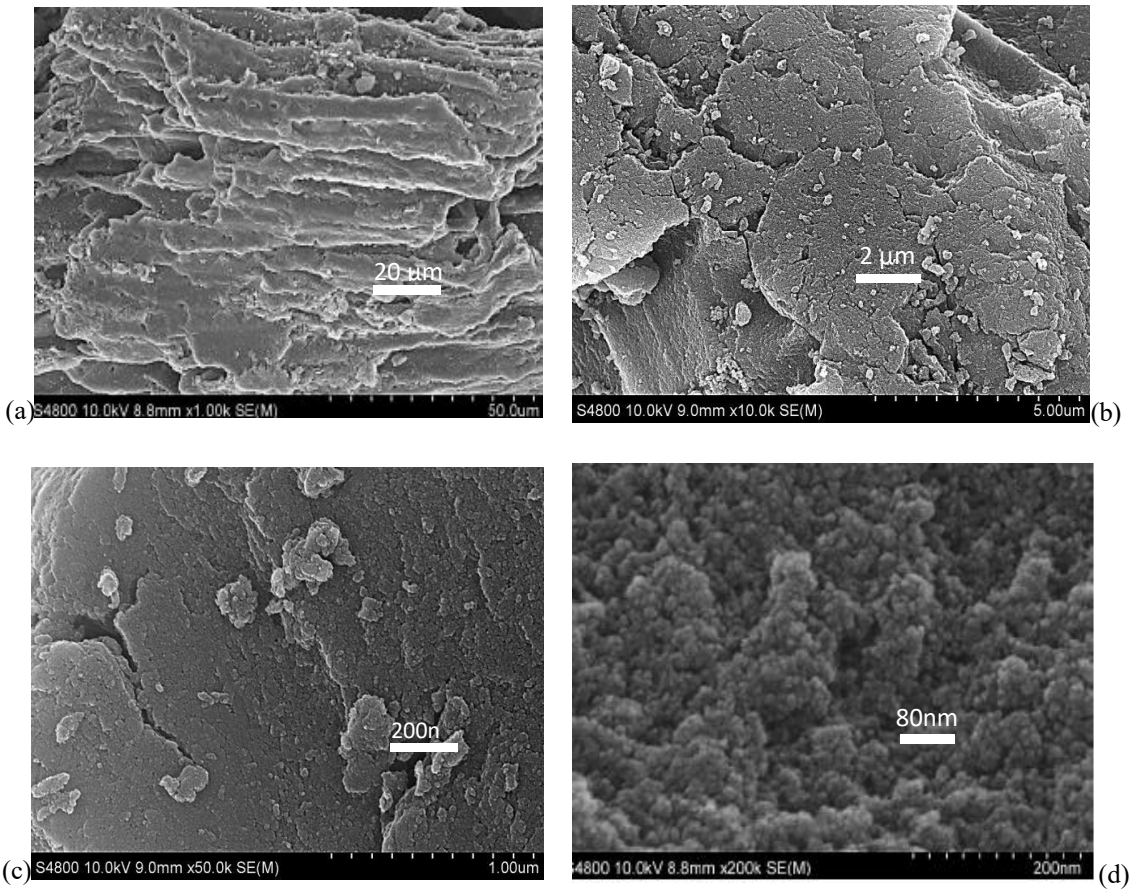

Figure 4: (a-d) SEM images of phosphoric acid impregnated *Buddleja* wood activated carbon (BWC_2.0), at different magnifications

High-resolution SEM images show that the H_3PO_4 can remove moisture and volatile organic components from the precursor during the carbonization, which develops disorderly arranged micro-pores and mesopores (Figure 4d). The SEM images suggested that the phosphoric acid reacted perfectly with the precursor to induce nanopores on the surface of activated carbon, useful for adsorbing pollutants from water by enhancing specific surface area and adsorption sites.

Dye Adsorption Isotherms

The adsorption capacity of the BWC_2.0 was analyzed by treating a synthetic methylene blue solution under different conditions (Figure 5). The time required to attain equilibrium of methylene blue adsorption was analyzed by measuring the adsorption percentage at different times (Figure 5a). More than 70% was adsorbed within 20 minutes, and the adsorption rate increased with time, reaching equilibrium by adsorbing 100% of the methylene blue within 2 hours (Figure 5a). This suggests 2 hours of contact time is required for the 100% adsorption of methylene blue from aqueous solution. The dependency of methylene blue adsorption on *pH* is shown in Figure 5b. The adsorption percentage was low at acidic pH, and it increased with increasing pH. Almost 100% of methylene blue was adsorbed at basic *pH*. As indicated by the pH_{pzc}, the activated carbon was positively charged below pH 6.85 due to protonation. At low *pH*, the cationic dye must compete with high concentrations of H^+ ions to form bonds with the surface-active sites. At high *pH*, the activated carbon was negatively charged and efficiently adsorbs the positively charged methylene blue, thereby removing 100% of it (Pradhananga *et al*., 2017).

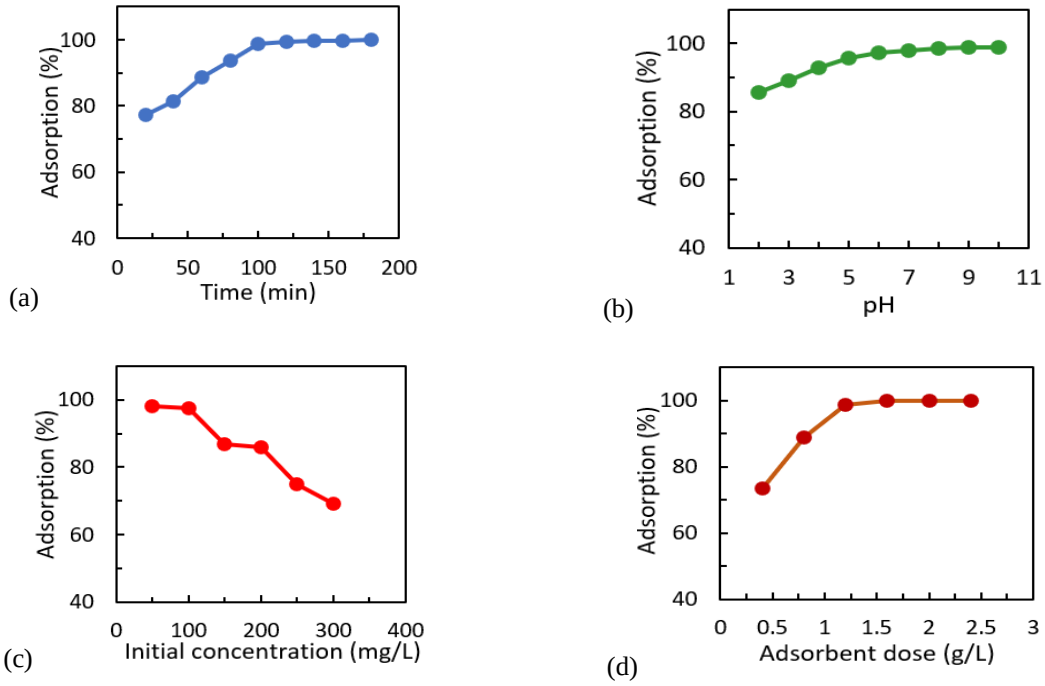

Figure 5: Dependence of methylene blue dye adsorption on (a) contact time, (b) *pH*, (c) concentration of methylene blue, and (d) dose of activated carbon

The adsorbing capacity of BWC-2.0 was determined by varying the concentration of methylene blue (Figure 5c). BWC-2.0 can remove almost completely (100%) up to 100 mg/L of methylene blue. Increasing the initial concentration, the adsorption percentage reduced to nearly 70% at 300 mg/L. Initially, the methylene blue adsorption capacity was high because there was a large availability of adsorption sites. As the concentration increased, the active sites of the adsorbate became occupied, resulting in a decrease in the adsorption percentage. The optimum amount of activated carbon required to remove 100 mg/L of methylene blue was studied by increasing the adsorbent dose from 0.5 to 2.5 g/L (Figure 5d). At low doses, the removal percentage was less than 90%. Further increasing the dose to 1.6 g/L, methylene blue was removed by 100%, suggesting 1.6 g/L was the optimum dose required to remove 100 mg/L of methylene blue.

The adsorption isotherm was studied by plotting linear and nonlinear curves (Figure 6). The q_e versus C_e plot shows an L-shaped curve (Figure 6a). Initially, the adsorption increases linearly due to the availability of vacant sites on the surface of activated carbon. Adsorption remains almost constant at high concentration, due to the saturation of adsorption sites, suggesting monolayer adsorption (Dimbo *et al.*, 2024).

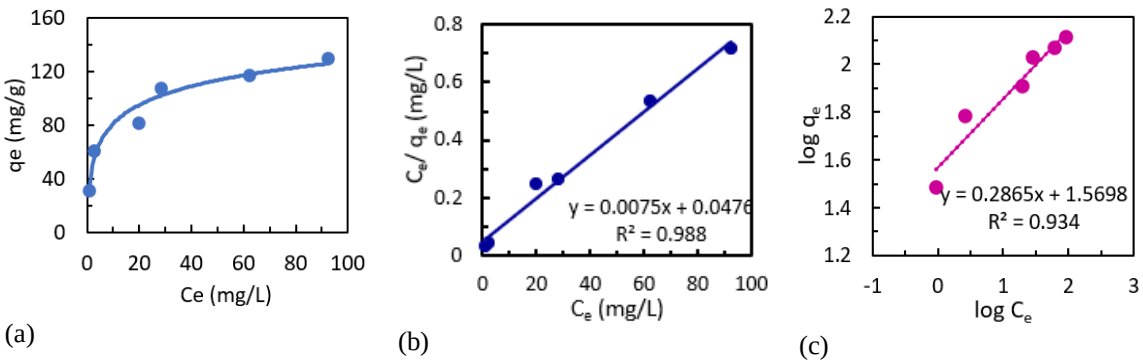

Figure 6: (a) Non-linear curve and linearized curve of (b) Langmuir and (c) Freundlich isotherms for methylene blue adsorption by BWC_2.0

Table 2: The Langmuir and the Freundlich parameters

Langmuir	Freundlich
q_{max} = 133.33 mg/g	K_F = 37.14 mg/g
b = 0.157 L/mg	n = 3.45
R^2 = 0.988	$1/n$ = 0.29
	R^2 = 0.934

From the linearized Langmuir and the Freundlich isotherms, the adsorption capacity of BWC-2.0 was determined (Figure 6b and 6c). A linear relationship between C_e and C_e/q_e with a coefficient of determination, R^2, of 0.988 was observed (Figure 6b, Table 2). The maximum adsorption of methylene blue was 133.33 mg/g, and the Langmuir constant, *b*, was 0.157 (Table 2). The excellent correlation suggests homogeneous monolayer adsorption of methylene blue (Adhikari & Bhatt, 2022). The Langmuir constant ($0 < 0.157 < 1$) suggested that this model is suitable for methylene blue adsorption. The Freundlich adsorption (Figure 6b) was represented by the linear relation of $logq_e$ and $logC_e$ with a coefficient of determination, R^2 of 0.934 (Table 2). The R^2 value for the Freundlich model was lower than that for the Langmuir model, which suggests the Langmuir isotherm model is more suitable for methylene blue adsorption on the BWC_2.0 activated carbon, i.e., there was ionic bonding between the negatively charged activated carbon and positively charged methylene blue (Amiri *et al.*, 2018). The q_{max} (133.33 mg/g) from the Langmuir model was comparable to the calculated q_e (140.84 mg/g, Figure 2b). The maximum methylene blue adsorption capacity obtained from the Langmuir model was 133.33 mg/g, which is higher than 86.207 mg/g for *Spathodea campanulata* (Dimbo *et al.*, 2024) and 19.09 mg/g for apricot stone-derived (Kavci *et al.*, 2021) activated carbon though it was lower than 312.5 mg/g of gram horse activated carbon (Adhikari & Bhatt, 2022).

Remediation of Polluted River Water

The direct discharge of effluent from households, industries, agricultural areas, etc., is continuously deteriorating river water in the core city area. Previous studies (Adhikari & Bhatt, 2022; Adhikari *et al.*, 2024; Mishra *et al.*, 2017; Sharma *et al.*, 2021) on the Bagmati River water concluded that the values of water quality parameters surpassed the WHO standard, suggesting the need for treatment of the river water before its use. The efficiency of BWC_2.0 was analyzed by treating Bagmati River water with it. The physicochemical characteristics of river water before and after treatment were tabulated in Table 3. The photographs of water before and after treatment are shown in Figure 7.

Figure 7: Photograph of water sample before (left) and after (right) treatment.

The sample water was black, but after treatment with BWC_2, it turned colorless, showing efficient removal of pollutants from the river water. Similarly, turbidity was 333 FNU before treatment and reduced to 13.7 FNU after treatment, which supports the color of the water (Figure 7).

Table 3: The concentrations of different parameters of river water

Parameters	**Before treatment**	**After treatment**	**WHO limit (WHO, 2011)**	**Removal (%)**
Color	black	Colorless	Colorless	
Turbidity (FNU)	333	13.7	<4	95.89
ORP (mV)	-214	75.9	-	135.47
Acidity (mg/L)	112.5	30.5	500	72.89
Alkalinity (mg/L)	360	55.5	200	84.58
pH	7.4	8.85	6.5-8.5	-19.59

Hardness (mg/L)	910	92	500	89.89
Conductivity (µS/cm)	823	775	1500	5.83
Sulfate (mg/L)	35.04	5.88	300	83.22
Phosphate (mg/L)	13.45	3.02	0.1	77.55
Nitrate ions (mg/L)	112.34	26.85	50	76.1
Chloride ions (mg/L)	188.15	72.775	<5	61.32
Iron (mg/L)	1.149	0.298	0.3	74.06
Chromium (mg/L)	1.716	0.231	0.05	86.54

The oxidation-reduction potential (ORP) indicates the ability to reduce pollutants. A high ORP value indicates the water contains a high concentration of dissolved oxygen required for bacteria to decompose dead cells and contaminants, hence removing pollutants from the water. Before treatments, the negative value of ORP (-214mV) indicated that there were excessive contaminants in the river water, causing an oxygen deficiency. Water containing low oxygen is unable to decompose contaminants and dead cells; hence, there is a lack of self-purification. The observed ORP was positive and very high (75.9 mV). This suggests that the BWC_2.0 removes not only suspended particles but also reduces contaminants from polluted water, hence enhancing dissolved oxygen. The chemical parameters, hardness, acidity, and alkalinity, sulfate, phosphate, nitrate, and chromate (chromium) ions were reduced from 70 to 90% by BWC_2.0 (Table 3) (Amosa, 2016; Kannan & Mani, 2014; Mkilima *et al.*, 2024). Although the percentage removal of turbidity, phosphate, chloride, and chromium ions was high, the values still exceeded the WHO-recommended standard. The presence of extremely high concentrations of pollutants saturated the available adsorption sites, and was unable to reduce all water quality parameters to below the recommended value. The chloride ion and iron were reduced up to 61.32% and 74.06 %, respectively. The conductivity of the river water was reduced by only 5.83% from 823 to 775 µS/cm, and pH was increased from 7.4 to 8.85 after treatment. The point of zero charge of BWC_2.0 was 6.85 (Table 1), *i.e.*, the surface of activated carbon will be negatively charged at pH higher than 6.85, and the negatively charged activated carbon can adsorb cations from aqueous solution. The activated carbon also reduced negatively charged contaminants from water after treatment. This may be due to the ion exchange mechanism, which releases hydroxide ions during interactions. The increase in pH after treatment is indicated by a negative value (-19.59) of % removal (Table 1), which may be due to the adsorption of cations, including H^+ ions, and the discharge of hydroxide ions, which increase pH and a small decrease in conductivity after treatment (Bhatangar *et al.*, 2013). The 84.58% reduction in alkalinity but only 5.83 % reduction in conductivity, with an increase in pH attributed to the adsorption of carbonate and bicarbonate ions, and release of OH^- ions after treatments with BWC_2.0. Most of the concentration of water quality parameters exceeded the WHO standard (WHO, 2011) before being treated with BWC_2.0; the values were reduced within the WHO-recommended limit after treatment. As indicated by Boehm titration, the acidic and basic functional groups of the activated carbon efficiently adsorb oppositely charged particles from river water (Adhikari & Bhatt, 2022; Amosa, 2016; Shi & Yao, 2011). The huge reduction of contaminants suggested that *Buddleja* wood activated carbon can be an effective application for the remediation of heavily polluted river water.

CONCLUSIONS

Buddleja wood activated carbons (BWCs) were prepared by activating with phosphoric acid. The pore size was quantitatively analysed from iodine and methylene blue numbers. The FTIR and Boehm titration suggested that phosphoric acid generated acidic and basic groups on the surface of activated carbon to adsorb anions and cations from aqueous solutions. The SEM images show amorphous particles of various sizes and shapes of activated carbon. The macro, meso, and micropores of different shapes and sizes of activated carbon adsorb foreign particles. The highest iodine (667 mg/g) and methylene blue (140 mg/g) numbers were found for activated carbons prepared with phosphoric acid to precursor ratio of 1:2.0 (BWC_2.0). The adsorption isotherms suggested that surface charges are responsible for the chemical adsorption of methylene blue following the Langmuir model. The physicochemical quality parameterization suggested that concentrations of most of the parameters exceeded the WHO-recommended values; however, after treatment with BWC_2.0,

contaminants, such as turbidity, ORP, acidity, alkalinity, hardness, sulphate, phosphate, nitrate, iron, and chromium, were reduced by more than 70%, though the values of turbidity, phosphate, chloride and chromium ions are still exceeded the WHO-recommended limits. Based on all the results, activated carbon from *Buddleja* wood can be used as an efficient adsorbent to reduce pollutants from extremely polluted water.

ACKNOWLEDGMENTS

The authors are thankful to Prof. Dr. Lok Kumar Shrestha and Sarita Manandhar MANA, NIMS, Japan, for FTIR data and SEM images essential for this research work. This research is supported by the University Grants Commission, Nepal, through the Collaborative Research Grant (CRG-79/80-S&T-01).

AUTHOR CONTRIBUTIONS

Conceptualization: MPA, NBA; Investigation: DS; Methodology: DS, MPA, NBA; Data curation: MPA; Data analysis: NBA; Writing - original draft: DS; Writing - review and editing: MPA, NBA.

CONFLICTS OF INTEREST

The authors declare no conflict of interest

DATA AVAILABILITY STATEMENT

The data used in this study are available from the corresponding author upon reasonable request.

REFERENCES

Adhikari, M. P., Rawal, N. B., Pradhananga, A. R., & Adhikari, N. B. (2024). Assessment of water quality index and role of tributaries on degradation of Bagmati river water. *Journal of Water and Environment Technology*, *22*(6), 255-270. https://doi.org/10.2965/jwet.23-118.

Adhikari, M. P., & Bhatt, J. R. (2022). Remediation of Bagmati River water using activated carbon from Macrotyloma uniflorum (gram horse) seed. *Bibechana*, *19*(1-2), 170-183.

Adhikari, M. P., & Thapa, A. (2020). Mn (II) adsorption on activated carbon derived from amaro (Spondias pinnata) seed stone. *Journal of Surface Science and Technology*, *36*(3-4), 147-159. DOI: 10.18311/jsst/2020/25657.

Adhikari, M. P., Nepal, B., Suwal, D., Manandhar, S., Shahi, S., Yadav, A. P., & Adhikari, N. B. (2025). Pistachio Shell-derived Activated Carbon as an Efficient Bio-adsorbent for River Water Treatment. *Journal of Institute of Science and Technology*, *30*(1), 57-64. https://doi.org/10.3126/jist.v30i1.73097.

Alazaiza, M. Y. D., Albahnasawi, A., Ali, G. A. M., Bashir, M. J. K., Nassani, D. E., Al Maskari, T., Amr, S. S. A., & Abujazar, M. S. S. (2022). Application of Natural Coagulants for Pharmaceutical Removal from Water and Wastewater: A Review. *Water*, *14*(2), 140. https://doi.org/10.3390/w14020140.

Amiri, M. J., Arshadi, M., Giannakopoulos, E., & Kalavrouziotis, I. K. (2018). Removal of mercury (II) and lead (II) from aqueous media by using a green adsorbent: kinetics, thermodynamic, and mechanism studies. *Journal of Hazardous, Toxic, and Radioactive Waste*, *22*(2), 04017026. httBW://doi.org/10.1061/(asce)hz.2153-5515.0000383.

Amosa, M. K. (2016). Sorption of water alkalinity and hardness from high-strength wastewater on bifunctional activated carbon: process optimization, kinetics and equilibrium studies. *Environmental Technology*, *37*(16), 2016-2039. https://doi.org/10.1080/09593330.2016.1139631.

APHA-AWWA-WEF: Standard Methods for Examination of Water and Wastewater, 22nd edition. (2012) American Public Health Association/American Water Works Association/Water Environment Federation, Washington, DC, USA.

Bhatnagar, A., Hogland, W., Marques, M., & Sillanpää, M. (2013). An overview of the modification methods of activated carbon for its water treatment applications. *Chemical Engineering Journal*, *219*, 499-511. https://doi.org/10.1016/j.cej.2012.12.03.

Boehm, H. P. (1994). Some aspects of the surface chemistry of carbon blacks and other carbons. *Carbon*, *32*(5), 759-769. https://doi.org/10.1016/0008-6223(94)90031-0.

Carrier, M., Loppinet-Serani, A., Denux, D., Lasnier, J. M., Ham-Pichavant, F., Cansell, F., & Aymonier, C. (2011). Thermogravimetric analysis as a new method to determine the lignocellulosic composition of biomass. *Biomass and Bioenergy*, *35*(1), 298-307. https://doi.org/10.1016/j.biombioe.2010.08.067.

Dias, M., Pinto, J., Henriques, B., Figueira, P., Fabre, E., Tavares, D., Vale, C., & Pereira, E. (2021). Nutshells as efficient biosorbents to remove cadmium, lead, and mercury from contaminated solutions. *International Journal of Environmental Research and Public Health*, *18*(4), 1580. https://doi.org/10.3390/ijerph18041580.

Dimbo, D., Abewaa, M., Adino, E., Mengistu, A., Takele, T., Oro, A., & Rangaraju, M. (2024). Methylene blue adsorption from aqueous solution

using activated carbon of *Spathodea campanulata*. *Results in Engineering*, *21*, 101910. https://doi.org/10.1016/j.rineng.2024.101910.

Hendrawan, Y., Sajidah, N., Umam, C., Fauzy, M. R., Wibisono, Y., & Hawa, L. C. (2019). Effect of carbonization temperature variations and activator agent types on activated carbon characteristics of Sengon wood waste (*Paraserianthes falcataria* (L.) Nielsen). In *IOP Conference Series: Earth and Environmental Science*, *239*(1), p. 012006). IOP Publishing. 012006. https://doi.org/10.1088/1755-1315/239/1/012006.

Kakom, S. M., Abdelmonem, N. M., Ismail, I. M., & Refaat, A. A. (2023). Activated carbon from sugarcane bagasse pyrolysis for heavy metals adsorption. *Sugar Tech*, *25*(3), 619-629. https://doi.org/10.1007/s12355-022-01214-3.

Kannan, D., & Mani, N. (2014). Removal of hardness (Ca^{2+}, Mg^{2+}) and alkalinity from ground water by low-cost adsorbent using *Phyllanthus emblica* wood. *International Journal of Chemical and Pharmaceutical Analysis*, *1*(4), 208-212.

Kavci, E., Erkmen, J., & Bingöl, M. S. (2023). Removal of methylene blue dye from aqueous solution using citric acid modified apricot stone. *Chemical Engineering Communications*, *210*(2), 165-180. https://doi.org/10.1080/00986445.2021.2009812.

Kuok, K. K., Chiu, P. C., Rahman, M. R., Chin, M. Y., & Bakri, M. K. B. (2024). Sustainable bamboo and coconut shell activated carbon for purifying river water on Borneo Island. *Waste Management Bulletin*, *2*(1), 39-48. https://doi.org/10.1016/j.wmb.2023.12.008.

Lund, T. (2019). Determination of the hardness of tap water using EDTA titration. *2*(27849.39527). https://doi. org/10.13140/RG.

Megherbi, H., Runtti, H., Tuomikoski, S., Heponiemi, A., Hu, T., Lassi, U., & Reffas, A. (2025). The effect of phosphoric acid on the properties of activated carbons made from Myrtus communis leaves: textural characteristics, surface chemistry, and capacity to adsorb Methyl orange. *Journal of Molecular Structure*, *1321*, 140038. https://doi.org/10.1016/j.molstruc.2024.140038.

Mishra, B. K., Regmi, R. K., Masago, Y., Fukushi, K., Kumar, P., & Saraswat, C. (2017). Assessment of Bagmati river pollution in Kathmandu Valley: Scenario-based modeling and analysis for sustainable urban development. *Sustainability of Water Quality and Ecology*, *9*, 67-77. https://doi.org/10.1016/j.swaqe.2017.06.001.

Mkilima, T., Zharkenov, Y., Abduova, A., Sarypbekova, N., Kirgizbayeva, K., Zhumadilov, I., ... & Zharassov, S. (2024). Investigating the potential of wheat straw and pistachio shell as a bio-functionalized agricultural waste biomass for enhanced biosorption of pollutants from wastewater. *Case Studies in Chemical and Environmental Engineering*, *9*, 100662. https://doi.org/10.1016/j.cscee.2024.100662.

Mutlu, E., & Kurnaz, A. (2017). Determination of seasonal variations of heavy metals and physicochemical parameters in Sakiz Pond (Kastamonu-Turkey). *Fresenius Environmental Bulletin*, *26*(4), 2806-2815.

Pereira, M. F. R., Soares, S. F., Órfão, J. J., & Figueiredo, J. L. (2003). Adsorption of dyes on activated carbons: influence of surface chemical groups. *Carbon*, *41*(4), 811-821. https://doi.org/10.1016/S0008-6223(02)00406-2.

Pradhananga, R. R., Adhikari, L., Shrestha, R. G., Adhikari, M. P., Rajbhandari, R., Ariga, K., & Shrestha, L. K. (2017). Wool carpet dye adsorption on nanoporous carbon materials derived from agro-product. *C*, *3*(2), 12. https://doi.org/10.3390/c3020012.

Saka, C. (2012). BET, TG–DTG, FT-IR, SEM, iodine number analysis and preparation of activated carbon from acorn shell by chemical activation with $ZnCl_2$. *Journal of Analytical and Applied Pyrolysis*, *95*, 21-24. https://doi.org/10.1016/j.jaap.2011.12.020.

Sathish, S., Vikram, S. & Suraj, R.J.N.E. (2018). Effectiveness of turbidity removal from synthetic and tannery wastewater by using seeds of a natural coagulant *Citrullus lanatus*. *Nature Environment and Pollution Technology*, *17*(2), 551-553.

Sharma, C. M., Shichang, K., Lekhendra, T., Rukumesh, P., & Mika, S. (2021). Major ions and irrigation water quality assessment of the Nepalese Himalayan rivers. *Environment, Development and Sustainability*, *23*(2), 2668-2680. DOI:10.1007/s10668-020-00694-1.

SHI, Z. L., LIU, F. M., & YAO, S. H. (2011). Adsorptive removal of phosphate from aqueous solutions using activated carbon loaded with Fe (III) oxide. *New carbon materials*, *26*(4), 299-306. https://doi.org/10.1016/S1872-5805(11)60083-8.

Shin, S., Jang, J., Yoon, S. H., & Mochida, I. (1997). A study on the effect of heat treatment on functional groups of pitch based activated carbon fiber using FTIR. *Carbon*, *35*(12), 1739-1743. https://doi.org/10.1016/S0008-6223(97)00132-2.

Sing, K. S. (1982). Reporting physisorption data for gas/solid systems with special reference to the determination of surface area and porosity (Provisional). *Pure and applied*

chemistry, *54*(11), 2201-2218. doi.org/10.1351/pac198254112201.

Tsolaki, E., & Diamadopoulos, E. (2010). Technologies for ballast water treatment: a review. *Journal of Chemical Technology & Biotechnology*, *85*(1), 19-32. https://doi.org/10.1002/jctb.2276.

Turin, M. (2003). Ethnobotanical notes on Thangmi plant names and their medicinal and ritual uses. *Contributions to Nepalese Studies*, *30*(1), 19-52.

Vali, I. P., Anusha, B. S., Pruthvija, M., Savitha, S., Ravindra, S., Nagaveni, M., ... & Swathi, N. (2024). Bamboo and coconut shell based activated carbon: a Raman spectroscopic study. *Materials Chemistry and Physics*, *318*, 129240. https://doi.org/10.1016/j.matchemphys.2024.129240.

World Health Organization "Guidelines for Drinking-Water Quality 4thed, World Health Organization, 2011, 20 Avenue Appia, 1211 Geneva 27, Switzerland.

Yuan, R., Guo, Y., Gurgan, I., Siddique, N., Li, Y-S., Jang, S., Noh, G. A. & Kim, S. H. (2025). Raman spectroscopy analysis of disordered and amorphous carbon materials: A review of empirical correlations. *Carbon*, 238, 120214. https://doi.org/10.1016/j.carbon.2025.120214